

Field Evaluation of Real-Time XBT Systems

Michael SZABADOS and Darren WRIGHT

*National Ocean Service, NOAA
6001 Executive Blvd
Rockville, MD 20852 - U.S.A.*

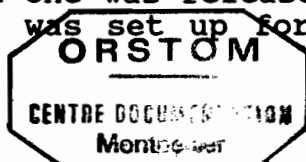
INTRODUCTION

The use of XBT's to measure the ocean's subsurface temperature has significantly increased over the past decade. NOAA is actively participating in an international effort to increase the number of subsurface temperature observations in support of global oceanographic and climate studies. NOAA's XBT program currently supports more than one hundred voluntary observing ships (VOS). These vessels are responsible for more than 12,000 XBT observations each year. Determining the field performance of XBT data systems is an importance step in the quality control of these data. The purpose of this field test was to evaluate the performance of four XBT systems under field conditions. The systems evaluated were a SEAS III (Sippican's MK-9), a Bathy Systems' 810 XBT Controller, an ARGOS XBT system, and Oregon State University's (OSU) XBT Data Box. In addition, the capability of both the ARGOS and GOES satellite systems to transmit XBT data in the JJXX format were evaluated. The SEAS III and ARGOS systems were used to evaluate the satellite transmission process for GOES and ARGOS respectively.

METHODS AND PROCEDURES

All XBT data were evaluated relative to a field standard. The field standard used was a Neil-Brown Instrument Systems Mark III CTD. Each XBT system and the Neil-Brown CTD were calibrated before and after the test. A decade box and XBT test canister were used to evaluate the XBT systems over a range of eleven resistance (temperature) values. The results of the XBT calibration check are presented in Table 1. Initially the OSU system failed the calibration test at temperatures below 5 degrees Celsius. The system was returned to the manufacturer for adjustments. The values from the OSU system in Table 1 were taken from a second calibration check of the OSU system after adjustments were made by the manufacturer.

The XBT Field Evaluation took place on board the NOAA Ship WHITING during July 1988. The WHITING was participating in studies of the current and water mass structure in the Southwestern North Atlantic Ocean in the context of the Subtropical Atlantic Climate Studies (STACS) Program. The evaluation occurred during the Barbados-Barbados leg of the cruise when thirty-three CTD casts were taken. Station locations are shown in Figure 1. During each CTD cast, two XBT's were released from each system. One was released during the descent of the CTD and one was released during the ascent of the CTD. Each XBT system was set up for an XBT drop prior to the



F 30766

descent of the CTD. To minimize the influence of internal waves, XBT's were released from each system at the same time when the CTD was located in the thermocline. Similar procedures were repeated during the ascent of the CTD. XBT's released during the ascent of the CTD were used to help indicate the temporal variability of the thermal structure while on station. Only XBT's released during the descent of the CTD were used for the XBT-CTD comparison. A total of 250 XBT's were released during the evaluation. Of these, 126 were released during the descent of the CTD. Table 2 presents the total number and type of XBT probe released for each system during the descent of the CTD. No T-5 or T-10 probes were used with the OSU and ARGOS system since these systems were not programmed with the corresponding depth coefficients.

Table 1. XBT SYSTEM CALIBRATION CHECK
(Temperature in Degrees Celsius)

<u>Resistance (Calibration Temp)</u>	<u>XBT System Temp - Calibration temp</u>			
	<u>MK-9</u>	<u>BATHY</u>	<u>OSU</u>	<u>ARGOS</u>
3193 (35.55)	0.00	-0.06	-0.05	**N/A
3350 (34.44)	-0.05	0.08	-0.08	**N/A
4024 (30.00)	0.02	0.13	-0.01	-0.03
5000 (25.00)	-0.01	0.08	-0.04	-0.06
6247 (20.00)	0.00	0.06	-0.05	-0.06
7274 (16.66)	0.01	0.05	-0.05	-0.06
9948 (10.00)	0.02	0.04	-0.05	-0.06
12679 (5.00)	0.03	0.04	-0.02	-0.03
16329 (0.00)	0.01	0.00	-0.05	-0.06
17287 (-1.10)	0.00	0.01	-0.06	-0.07
18094 (-2.00)	0.01	0.00	-0.04	-0.05

** - The ARGOS system does not handle temperatures in these two ranges.

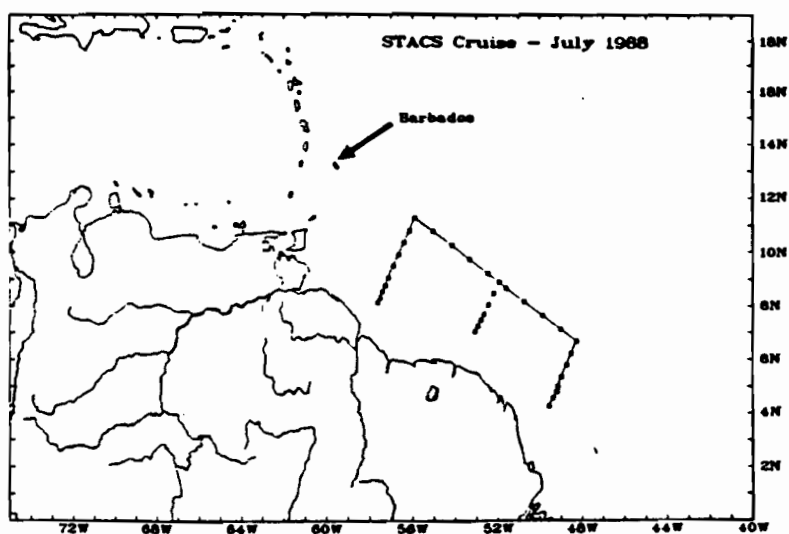


Figure 1. Cruise Track and XBT/CTD Stations

Table 2. PROBE TYPE AND NUMBER RELEASED FOR EACH XBT SYSTEM DURING DESCENT OF CTD

<u>PROBE TYPE</u>	<u>MK-9</u>	<u>BATHY</u>	<u>OSU</u>	<u>ARGOS</u>
T-10	7	7	0	0
T-7	7	7	7	7
T-6	7	7	15	15
T-5	5	5	0	0
T-4	7	7	8	8

Out of the 250 XBT's released, there were a total of five probe failures (2%). A summary of common XBT malfunctions is presented in Kroner and Blumenthal, 1978. The BATHY system had one probe failure, while the OSU and ARGOS systems each had two probe failures. Five software/system crashes occurred with the OSU system. These failures were attributed to incompatibility between the OSU software and the PC clone (televideo XL computer) used. All XBT data collected by the SEAS III and the ARGOS systems were transmitted in real-time contingent on available space in the satellite transmission window.

Before comparing the XBT data to the CTD data, XBT depth-temperature pairs were computed using a linear interpolation scheme so as to have the XBT depth coincide with the CTD depth. Except for the profile plots comparing the XBT and CTD traces, analysis was based on the interpolated XBT data.

RESULTS

Several factors must be considered in the evaluation of XBT - CTD temperature comparisons. Some of the important factors are the methods used to determine the depth of the XBT and the CTD, thermistor errors, and environmental factors such as the stability of the water column. Differences between a temperature measured by the CTD and an XBT can in part be attributed to the computation of the XBT probe depth. The depth of the XBT is determined by using a depth equation based on the fall rate of the probe, while the CTD depth is measured using a pressure transducer. In addition, the XBT descends at a faster rate than the CTD (6.5 m/sec, XBT; 0.5 m/sec, CTD). The XBT and CTD will therefore measure temperature simultaneously at the same depth and time only once. Any changes in the thermal structure of the water column during the descent of the CTD due to internal waves will appear as a temperature difference between the CTD and XBT. Temperature differences between an XBT system and the CTD can also be attributed to the individual thermistor in each XBT probe. While each XBT system and the CTD thermistor were calibrated, the actual thermistor in each XBT probe were not.

The mean of the absolute temperature difference between the CTD and each XBT system over the total XBT profile for each probe type is provided in Table 3. These results show differences greater than the +/- 0.15 degree Celsius specification for XBT probes. To interpret these results it is important to identify the factors which contribute to these differences between the XBT and CTD measurements.

Table 3. MEAN OF THE ABSOLUTE DIFFERENCE BETWEEN THE XBT AND CTD TEMPERATURE (Degrees Celsius)

SYSTEM	Probe Type									
	T-04		T-05		T-06		T-07		T-10	
	Mean	SD	Mean	SD	Mean	SD	Mean	SD	Mean	SD
MK-9	.36	.14	.11	.06	.33	.13	.34	.24	.30	.21
BATHY	.30	.15	.24	.17	.26	.11	.30	.19	.33	.18
OSU	.19	.19			.14	.06	.18	.07		
ARGOS	.38	.22			.39	.11	.42	.33		

To isolate the contributions of the XBT thermistor error to the results shown in Table 3, temperature differences in the isothermal portion of the mixed layers were analyzed. This was done because temperature differences due to depth errors, instrument response, and internal waves would be minimized by these conditions. Thus, as shown in Table 4, when comparing only temperatures in the isothermal portion of the mixed layers, the temperature difference between the CTD and all four systems was reduced by an order of magnitude. The mean departure of the XBT temperature from that of the CTD is well within the XBT specifications. These results also agree well with the XBT system calibration check in Table 1.

Table 4. MEAN TEMPERATURE DIFFERENCES BETWEEN THE XBT AND CTD IN THE MIXED LAYERS (DEGREES CELSIUS)

SYSTEM	MEAN	STANDARD DEVIATION
MK-9	.029	.046
BATHY	.106	.064
OSU	-.074	.083
ARGOS	.016	.055

Errors in XBT depth can also contribute to the differences found between the XBT and CTD temperatures. The temperature profiles in Figure 2 show a depth offset between the XBT and CTD data. To determine the associated XBT temperature error due to an offset in XBT depth, the XBT data was shifted in depth to find a best fit with the CTD data. A best fit of the XBT profile to the CTD was found by shifting the XBT data in 50 meter segments by one-meter increments up and down until the least mean difference between the XBT and CTD temperatures was determined. The depth error was then

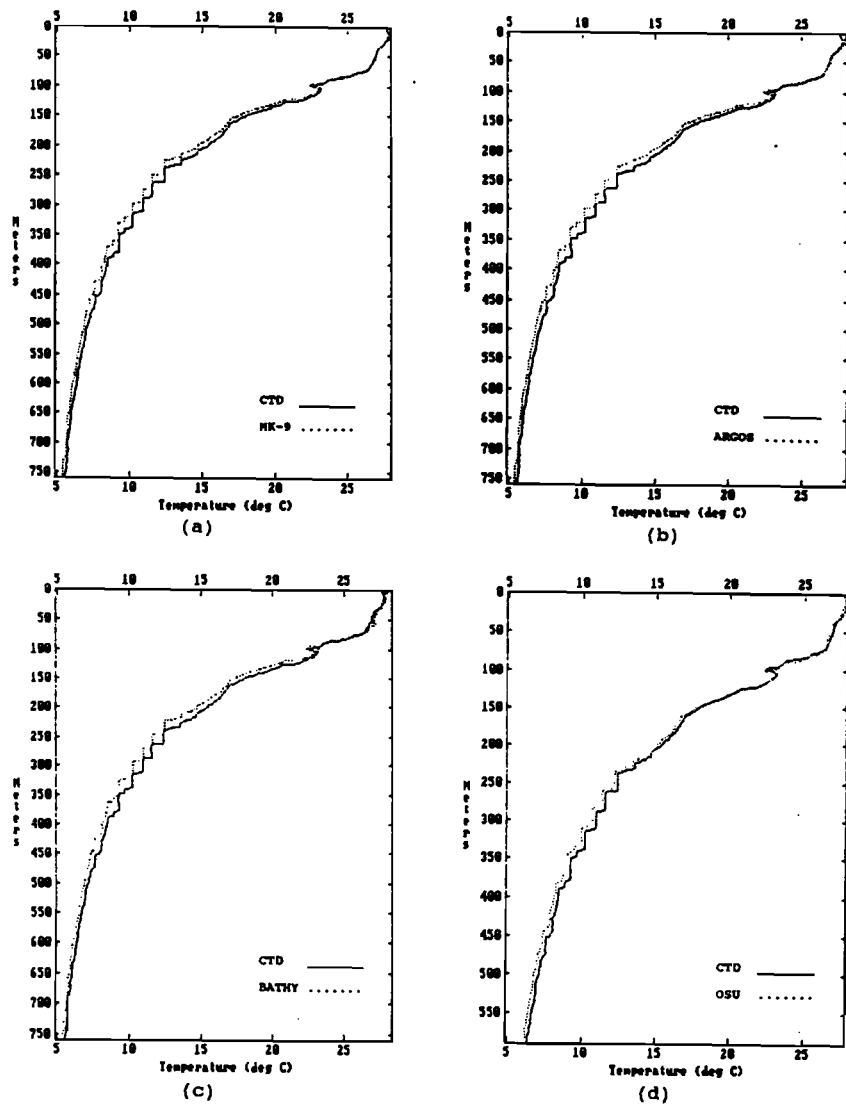


Figure 2. XBT - CTD Temperature Profiles, XBT Drop 25.
 (a) MK-9 (b) ARGOS (c) BATHY (d) OSU

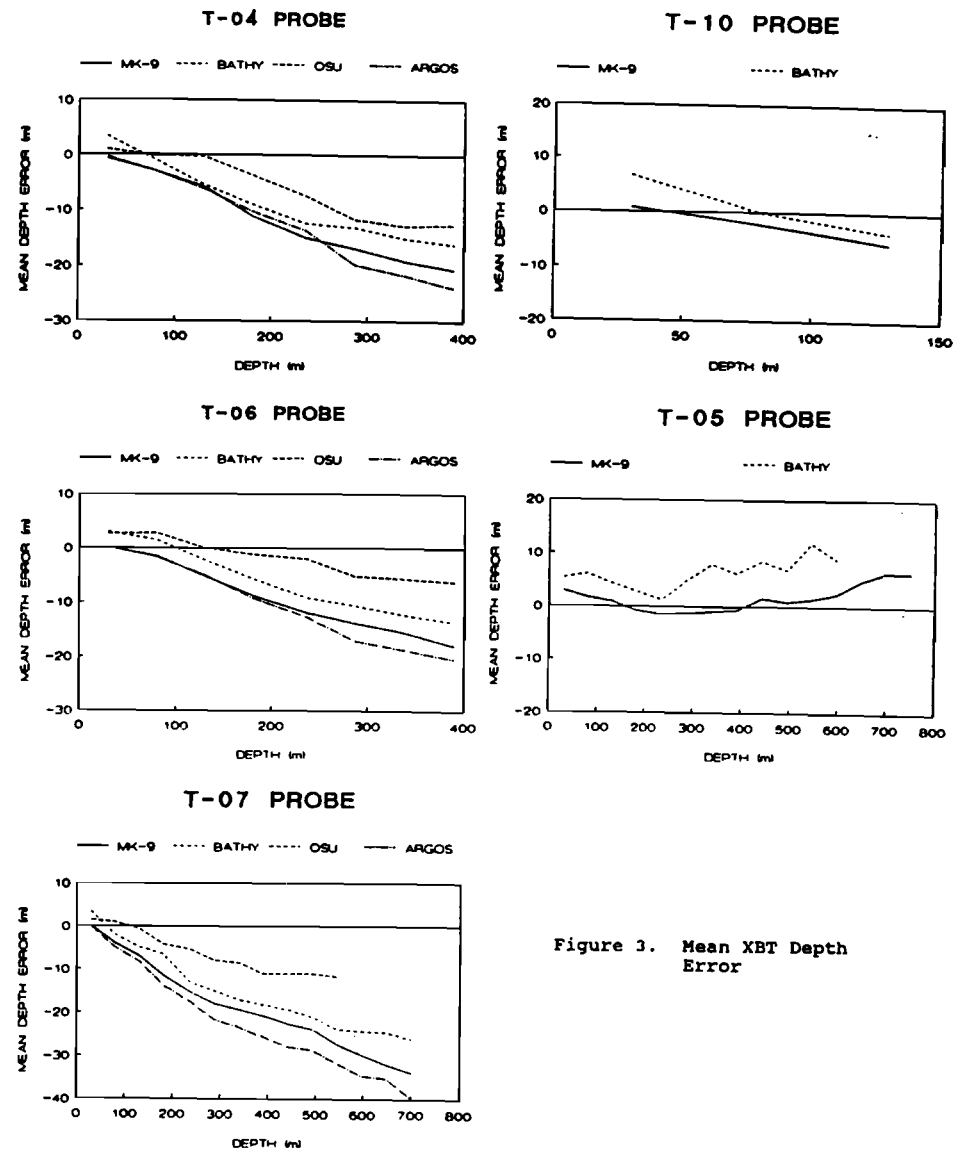


Figure 3. Mean XBT Depth Error

computed from how many meters the original XBT data was moved to best fit the CTD data. Table 5 provides a sample output from this analysis. As is shown in Table 5, by shifting the XBT depth the temperature difference between the XBT and CTD can be reduced by an order of magnitude. The mean temperature difference with a depth correction agrees well with the temperature difference found in the mixed layers and those from the calibration check.

For each of the XBT systems, the mean depth error in 50 meter segments is shown in Figure 3 by probe type. While there appears to be some bias between different XBT systems, it is important to note that for all the XBT systems the depth error for probe types T-4, T-6, and T-7 show a similar trend. This trend indicates that these XBT probe types are falling at a faster rate than calculated by the XBT depth equation, using the standard coefficients. The standard depth equation and coefficients are provided in Table 6 (Sippican, 1973). Similarly, the T-10 probes are falling at a faster rate, while the T-5 probes are falling at the proper rate. The OSU system depth error, as shown in Figure 3, was less than the other systems. This resulted in a smaller temperature difference from the CTD data as was indicated in Table 3.

Table 5. BEST-FIT ANALYSIS

System type: MK-9 Drop Number 27 Probe Type T-07

Depth Range (meters)	Depth Error (meters)	Mean Temp. Error w/ Depth Corrected (C)	Mean Temp. Error w/ Depth Uncorr. (C)
5.0 to 52.7	- 0.99	0.05 +/- 0.03	0.07 +/- 0.04
56.7 to 104.4	- 3.98	0.09 +/- 0.05	0.45 +/- 0.10
108.4 to 156.1	- 6.96	0.11 +/- 0.07	0.63 +/- 0.08
160.0 to 207.7	-10.93	0.05 +/- 0.05	0.62 +/- 0.10
211.7 to 259.4	-17.88	0.04 +/- 0.04	0.68 +/- 0.14
263.4 to 311.0	-19.86	0.02 +/- 0.03	0.49 +/- 0.10
315.0 to 362.7	-21.84	0.03 +/- 0.02	0.37 +/- 0.12
366.6 to 414.3	-24.82	0.03 +/- 0.02	0.48 +/- 0.07
418.2 to 465.9	-27.79	0.04 +/- 0.02	0.32 +/- 0.07
469.8 to 517.5	-30.76	0.04 +/- 0.02	0.32 +/- 0.03
521.4 to 569.0	-33.73	0.04 +/- 0.02	0.35 +/- 0.04
573.0 to 620.6	-41.65	0.03 +/- 0.02	0.35 +/- 0.02
624.6 to 672.2	-48.58	0.01 +/- 0.02	0.31 +/- 0.02
676.1 to 723.7	-49.56	0.03 +/- 0.02	0.22 +/- 0.02

Table 6. STANDARD FORM OF THE DROP EQUATION

Probe type	Coefficients		Depth= A*T - B*T ² (meters) T= sample rate * sample no.
	A	B	
T-4	6.472	.00216	
T-5	6.828	.00182	
T-6	6.472	.00216	
T-7	6.472	.00216	
T-10	6.301	.00216	

To determine if the XBT depth for the T-4, T-6, and T-7 probes could be corrected by modifying the coefficient in the depth equation, a regression analysis was employed to revise the coefficients using the MK-9 data. This was accomplished by first calculating what the sample interval would have to be to provide the correct depth as determined by the best fit analysis. This sample interval was found to be 0.105 seconds. The actual MK-9 sample interval is 0.1 seconds. The revised coefficients A' and B' were then determined by the following method:

$$A' = (6.472 * 0.105) / 0.1 = 6.796$$

$$B' = (0.00216 * (0.105)^2) / 0.01 = 0.00238$$

New temperature and depth pairs for the T-4, T-6, and T-7 probes using the revised coefficients were then computed. Scatter plots comparing the XBT and CTD using the standard and revised coefficients are presented in Figure 4. As shown in these plots the revised coefficients improve the agreement between the XBT and CTD temperature data. Using the same revised coefficients, the ARGOS and BATHY data had similar results. The temperature profiles that were shown in Figure 2 are replotted in Figure 5 using the revised coefficients. Most of the temperature errors associated with the depth offset (previously characterized by the temperature profiles in Figure 2) are now reduced or eliminated. The exception is the OSU XBT data which has better agreement with the CTD data using the standard coefficients.

To determine the temporal variability of the water column during the XBT-CTD comparison, XBT's were launched from each system during the ascent of the CTD. This provided a measure of the variability on the scale of one hour. Any variability on this time scale is likely a result of internal waves. While a few stations exhibited variability in the thermocline of about 10 meters, typically the variability was less than 2 meters. To quantitatively determine the influence of internal waves on the CTD - XBT comparison, several more XBT drops are required during the descent of the CTD. Although variability of the water column due to internal waves can influence the comparison between the XBT and CTD, it should be minimal since it takes approximately 16 minutes for the CTD to reach 500 meters.

The real-time transmission of XBT data is crucial to the optimum utilization of these data sets by the oceanographic and climatological communities. The alternative is retrospective data submission to national data archives which historically can take months, years or even worse never. During the field test the ARGOS and GOES satellite systems were evaluated for their XBT data transmission capability using the SEAS III and ARGOS XBT systems, respectively. For both these systems, data received was disseminated to the community on the Global Telecommunication System (GTS).

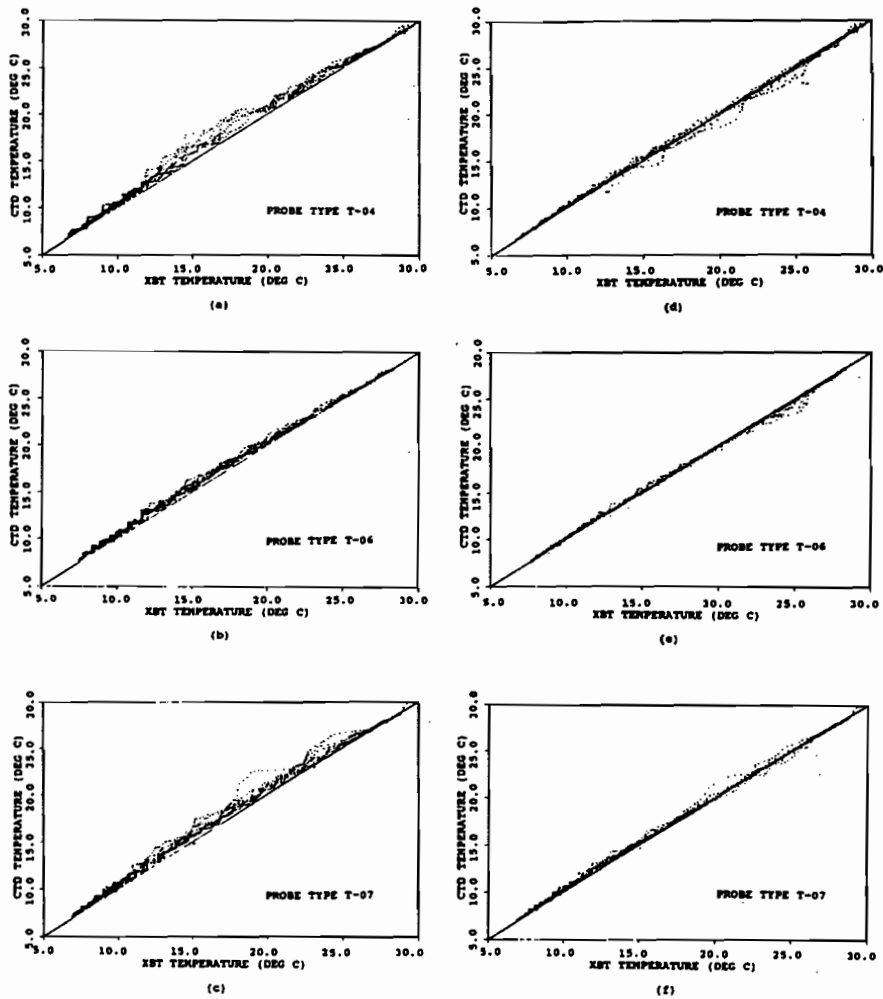


Figure 4. Scatter Plots of MK-9 XBT Data vs. Ctd Data
 (a-c) Standard Depth Coefficients
 (d-f) Revised Depth Coefficients

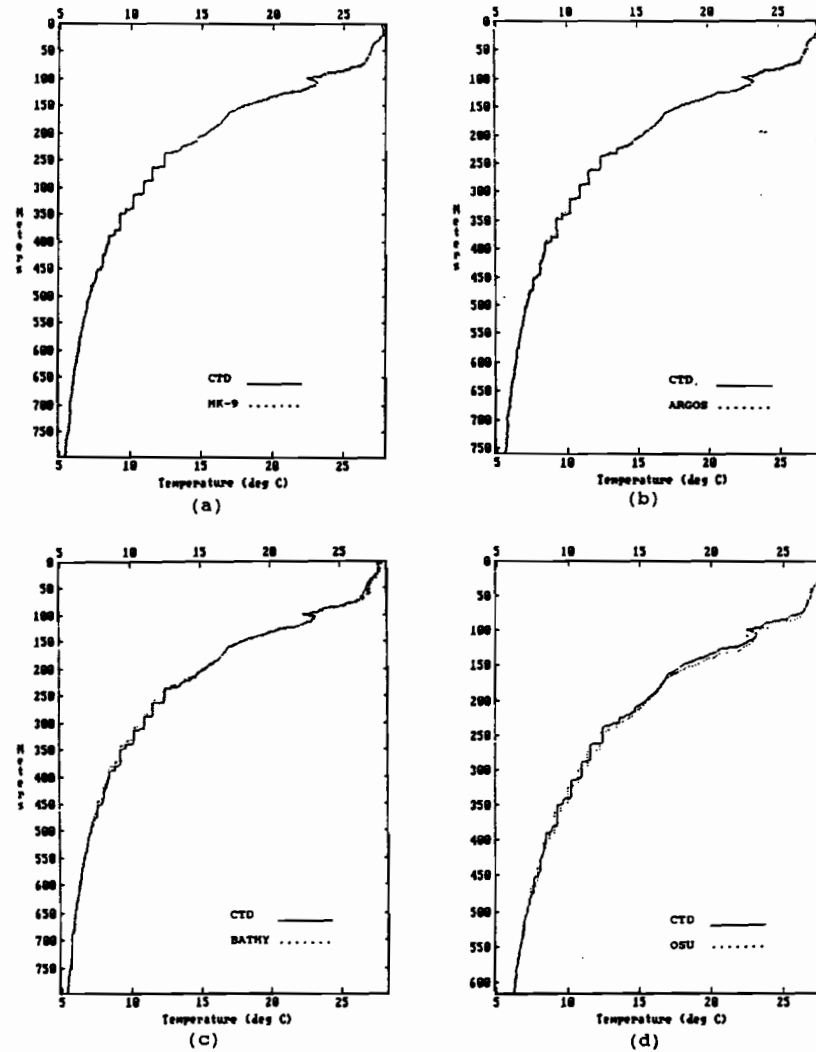


Figure 5. XBT -CTD Temperature Profiles, XBT Drop 25
 with Revised Depth Coefficients.
 (a) MK-9 (b) ARGOS (c) BATHY (d) OSU

Table 7 summarizes the results from evaluating the real-time data transmissions. Of the 60 XBT's dropped using the ARGOS XBT system, 48 XBT messages were transmitted. Ten were not transmitted because of the 15 iteration limit, imposed by the software in version 1.0, to compute the 15 inflection points. This limitation has been corrected in version 2.0. Two XBT messages were not transmitted because of faulty probes. The high launch frequency, sometimes generating a message every hour, resulted in 11 of the 48 messages not being generated into GTS bulletins. The bulletins were not generated because of the required two transmission receptions not being received. This should not be considered a limitation of the system since most oceanographic surveys do not require the high XBT launch frequency used during this field test. Of the 65 XBT's dropped using the SEAS III system, 58 XBT messages were transmitted and entered onto the GTS. Seven of the XBT drops were not transmitted because of the high frequency of XBT launches. The XBT buffer in the GOES transmitter allows for 3 XBT messages. Since the GOES satellite assignment permitted a transmission every 4 hours, the XBT transmitter rejected seven XBT drops. Again, most oceanographic surveys do not require this high frequency of XBT launches. If necessary, the data can be stored on floppy disk and transmitted at a later time.

TABLE 7 SUMMARY OF REAL-TIME DATA TRANSMISSION

<u>SYSTEM</u>	<u>XBT's DROPPED</u>	<u>TRANSMISSION STATUS</u>	<u>DATA DISSEMINATION STATUS</u>
ARGOS	60	Transmitted - 48 Not Transmitted - 10 (1) Not Transmitted - 2 (2)	Data Bulletins - 37 Not Disseminated - 11 (3)
SEAS III	65	Transmitted - 58 Not Transmitted - 7 (3)	Data Bulletins - 58

-
- (1) Ten XBT messages not generated because criteria for obtaining 15 inflections points were too strict. This limitation is corrected in latest software, Version 2.0.
 - (2) Two XBT messages not generated because of XBT probe failure.
 - (3) Eleven from the ARGOS XBT system and 7 from the SEAS III system were neither transmitted or disseminated in real-time because of the high launch frequency during field evaluation.

SUMMARY

This field test evaluated both the performance of XBT systems under field conditions and the capability of the ARGOS and GOES satellite systems to transmit XBT data in the JJXX format. Results show that the mean temperature differences between the CTD and each XBT system over the total XBT profile were greater than the ± 0.15 degrees Celsius specification for XBT probes. In the isothermal portion of the mixed layer where the temperature differences between the XBT and CTD are minimized due to depth, instrument response, and internal waves, the temperature differences between the XBT's and CTD were reduced by an order of magnitude. From these results, it was determined that temperature error due to the XBT's thermistor is small. The major contributing factor for the differences in temperature is an error in the computation of the XBT probe depth. The error in depth for the T-4, T-6, and T-7 probe types was found to be greater than allowable by the manufacturer's specifications (± 5 meters or $\pm 2\%$ of depth, whichever is greater). It was determined that these probes are falling at a faster rate than calculated by the standard coefficient of the drop equation. This depth error has been previously identified by Heinmiller et al. (1983) and Seaver and Kuleshov (1982). The depth errors can be reduced by revising the coefficients in the depth equation. While all XBT systems indicated a depth error, there was a system bias among the systems, some showing a greater error than others. This bias among system requires further analysis. Transmission results demonstrated that both ARGOS and GOES satellite based XBT systems provided adequate capability to transmit data in real-time. Together, ARGOS and GOES provide the necessary data communications for a global ocean observation program.

ACKNOWLEDGEMENTS

We would like to express our sincere thanks to Sonny Richardson for help making this evaluation possible and for all his helpful suggestions. We'd like to thank Yvonne Newmen for helping with the data processing and preparation of this report. Also we appreciate the help, suggestions, and support of the following people, Archie Shaw and Mitch Tiger of Argos, Rod Mesecar and Jim Wagner of Oregon State University, Jim Hannon of Sippican, Don Dorson of Bathy Systems, Mike Miyake of the Institute of Ocean Sciences and Bob Molinari of NOAA/AOML.

REFERENCES

Seaver, G.A., Kuleshov, S., "Experimental and Analytical Error of the Expendable Bathythermograph." *Journal of Physics and Oceanography*, 12, 592-600, 1982.

Heinmiller, R.H., Ebbesmeyer, C.C., Taft, B.A., Olson, D.B. and Nikitin, O.P., "Systematic Errors in Expendable Bathythermograph (XBT) Profiles." *Deep Sea Research*, 30, 1185-1197, 1983.

Kroner, S.M., Blumenthal, B.P., "Guide to Common Shipboard Expendable Bathythermograph (SXBT) Recording Malfunctions." *Naval Oceanographic Office*, August 1978.

Sippican Ocean Systems, "Operation/Maintenance Manual MK-9 Digital XBT/XSV System." September 1983.

**WESTERN PACIFIC INTERNATIONAL MEETING
AND WORKSHOP ON TOGA COARE**

Nouméa, New Caledonia

May 24-30, 1989

PROCEEDINGS

edited by

Joël Picaut *

Roger Lukas **

Thierry Delcroix *

* ORSTOM, Nouméa, New Caledonia

** JIMAR, University of Hawaii, U.S.A.

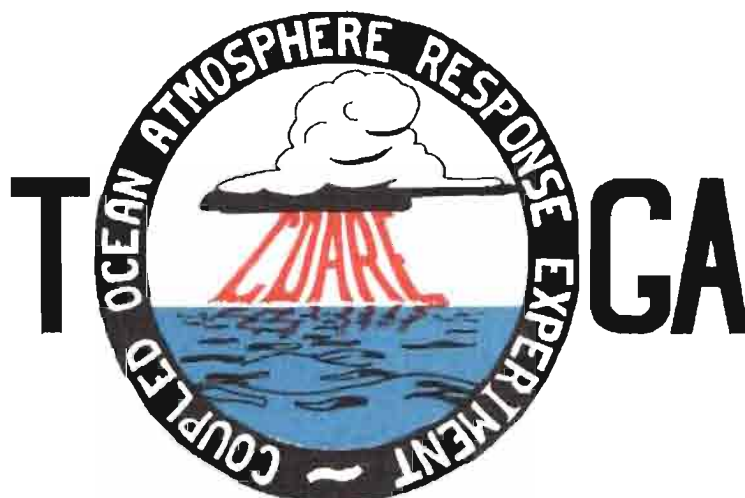


TABLE OF CONTENTS

ABSTRACT	i
RESUME	iii
ACKNOWLEDGMENTS	vi
INTRODUCTION	
1. Motivation	1
2. Structure	2
LIST OF PARTICIPANTS	5
AGENDA	7
WORKSHOP REPORT	
1. Introduction	19
2. Working group discussions, recommendations, and plans	20
a. Air-Sea Fluxes and Boundary Layer Processes	20
b. Regional Scale Atmospheric Circulation and Waves	24
c. Regional Scale Oceanic Circulation and Waves	30
3. Related programs	35
a. NASA Ocean Processes and Satellite Missions	35
b. Tropical Rainfall Measuring Mission	37
c. Typhoon Motion Program	39
d. World Ocean Circulation Experiment	39
4. Presentations on related technology	40
5. National reports	40
6. Meeting of the International Ad Hoc Committee on TOGA COARE	40
APPENDIX: WORKSHOP RELATED PAPERS	
Robert A. Weller and David S. Hosom: Improved Meteorological Measurements from Buoys and Ships for the World Ocean Circulation Experiment	45
Peter H. Hildebrand: Flux Measurement using Aircraft and Radars	57
Walter F. Dabberdt, Hale Cole, K. Gage, W. Ecklund and W.L. Smith: Determination of Boundary-Layer Fluxes with an Integrated Sounding System	81

MEETING COLLECTED PAPERS

WATER MASSES, SEA SURFACE TOPOGRAPHY, AND CIRCULATION

Klaus Wyrtki: Some Thoughts about the West Pacific Warm Pool	99
Jean René Donguy, Gary Meyers, and Eric Lindstrom: Comparison of the Results of two West Pacific Oceanographic Expeditions FOC (1971) and WEPOCS (1985-86)	111
Dunxin Hu, and Maochang Cui: The Western Boundary Current in the Far Western Pacific Ocean	123
Peter Hacker, Eric Firing, Roger Lukas, Philipp L. Richardson, and Curtis A. Collins: Observations of the Low-latitude Western Boundary Circulation in the Pacific during WEPOCS III	135
Stephen P. Murray, John Kindle, Dharma Arief, and Harley Hurlburt: Comparison of Observations and Numerical Model Results in the Indonesian Throughflow Region	145
Christian Henin: Thermohaline Structure Variability along 165°E in the Western Tropical Pacific Ocean (January 1984 - January 1989)	155
David J. Webb, and Brian A. King: Preliminary Results from Charles Darwin Cruise 34A in the Western Equatorial Pacific	165
Warren B. White, Nicholas Graham, and Chang-Kou Tai: Reflection of Annual Rossby Waves at The Maritime Western Boundary of the Tropical Pacific	173
William S. Kessler: Observations of Long Rossby Waves in the Northern Tropical Pacific	185
Eric Firing, and Jiang Songnian: Variable Currents in the Western Pacific Measured During the US/PRC Bilateral Air-Sea Interaction Program and WEPOCS	205
John S. Godfrey, and A. Weaver: Why are there Such Strong Steric Height Gradients off Western Australia ?	215
John M. Toole, R.C. Millard, Z. Wang, and S. Pu: Observations of the Pacific North Equatorial Current Bifurcation at the Philippine Coast	223

EL NINO/SOUTHERN OSCILLATION 1986-87

Gary Meyers, Rick Bailey, Eric Lindstrom, and Helen Phillips: Air/Sea Interaction in the Western Tropical Pacific Ocean during 1982/83 and 1986/87	229
Laury Miller, and Robert Cheney: GEOSAT Observations of Sea Level in the Tropical Pacific and Indian Oceans during the 1986-87 El Nino Event	247
Thierry Delcroix, Gérard Eldin, and Joël Picaut: GEOSAT Sea Level Anomalies in the Western Equatorial Pacific during the 1986-87 El Nino, Elucidated as Equatorial Kelvin and Rossby Waves	259
Gérard Eldin, and Thierry Delcroix: Vertical Thermal Structure Variability along 165°E during the 1986-87 ENSO Event	269
Michael J. McPhaden: On the Relationship between Winds and Upper Ocean Temperature Variability in the Western Equatorial Pacific	283

John S. Godfrey, K. Ridgway, Gary Meyers, and Rick Bailey: Sea Level and Thermal Response to the 1986-87 ENSO Event in the Far Western Pacific	291
Joël Picaut, Bruno Camusat, Thierry Delcroix, Michael J. McPhaden, and Antonio J. Busalacchi: Surface Equatorial Flow Anomalies in the Pacific Ocean during the 1986-87 ENSO using GEOSAT Altimeter Data	301

THEORETICAL AND MODELING STUDIES OF ENSO AND RELATED PROCESSES

Julian P. McCreary, Jr.: An Overview of Coupled Ocean-Atmosphere Models of El Nino and the Southern Oscillation	313
Kensuke Takeuchi: On Warm Rossby Waves and their Relations to ENSO Events	329
Yves du Penhoat, and Mark A. Cane: Effect of Low Latitude Western Boundary Gaps on the Reflection of Equatorial Motions	335
Harley Hurlburt, John Kindle, E. Joseph Metzger, and Alan Wallcraft: Results from a Global Ocean Model in the Western Tropical Pacific	343
John C. Kindle, Harley E. Hurlburt, and E. Joseph Metzger: On the Seasonal and Interannual Variability of the Pacific to Indian Ocean Throughflow	355
Antonio J. Busalacchi, Michael J. McPhaden, Joël Picaut, and Scott Springer: Uncertainties in Tropical Pacific Ocean Simulations: The Seasonal and Interannual Sea Level Response to Three Analyses of the Surface Wind Field	367
Stephen E. Zebiak: Intraseasonal Variability - A Critical Component of ENSO ?	379
Akimasa Sumi: Behavior of Convective Activity over the "Jovian-type" Aqua-Planet Experiments	389
Ka-Ming Lau: Dynamics of Multi-Scale Interactions Relevant to ENSO	397
Pecheng C. Chu and Roland W. Garwood, Jr.: Hydrological Effects on the Air-Ocean Coupled System	407
Sam F. Iacobellis, and Richard C.J. Somerville: A one Dimensional Coupled Air-Sea Model for Diagnostic Studies during TOGA-COARE	419
Allan J. Clarke: On the Reflection and Transmission of Low Frequency Energy at the Irregular Western Pacific Ocean Boundary - a Preliminary Report	423
Roland W. Garwood, Jr., Pecheng C. Chu, Peter Muller, and Niklas Schneider: Equatorial Entrainment Zone : the Diurnal Cycle	435
Peter R. Gent: A New Ocean GCM for Tropical Ocean and ENSO Studies	445
Wasito Hadi, and Nuraini: The Steady State Response of Indonesian Sea to a Steady Wind Field	451
Pedro Ripa: Instability Conditions and Energetics in the Equatorial Pacific	457
Lewis M. Rothstein: Mixed Layer Modelling in the Western Equatorial Pacific Ocean	465
Neville R. Smith: An Oceanic Subsurface Thermal Analysis Scheme with Objective Quality Control	475
Duane E. Stevens, Qi Hu, Graeme Stephens, and David Randall: The hydrological Cycle of the Intraseasonal Oscillation	485
Peter J. Webster, Hai-Ru Chang, and Chidong Zhang: Transmission Characteristics of the Dynamic Response to Episodic Forcing in the Warm Pool Regions of the Tropical Oceans	493

MOMENTUM, HEAT, AND MOISTURE FLUXES BETWEEN ATMOSPHERE AND OCEAN

W. Timothy Liu: An Overview of Bulk Parametrization and Remote Sensing of Latent Heat Flux in the Tropical Ocean	513
E. Frank Bradley, Peter A. Coppin, and John S. Godfrey: Measurements of Heat and Moisture Fluxes from the Western Tropical Pacific Ocean	523
Richard W. Reynolds, and Ants Leetmaa: Evaluation of NMC's Operational Surface Fluxes in the Tropical Pacific	535
Stanley P. Hayes, Michael J. McPhaden, John M. Wallace, and Joël Picaut: The Influence of Sea-Surface Temperature on Surface Wind in the Equatorial Pacific Ocean	543
T.D. Keenan, and Richard E. Carbone: A Preliminary Morphology of Precipitation Systems In Tropical Northern Australia	549
Phillip A. Arkin: Estimation of Large-Scale Oceanic Rainfall for TOGA	561
Catherine Gautier, and Robert Frouin: Surface Radiation Processes in the Tropical Pacific	571
Thierry Delcroix, and Christian Henin: Mechanisms of Subsurface Thermal Structure and Sea Surface Thermo-Haline Variabilities in the South Western Tropical Pacific during 1979-85 - A Preliminary Report	581
Greg. J. Holland, T.D. Keenan, and M.J. Manton: Observations from the Maritime Continent : Darwin, Australia	591
Roger Lukas: Observations of Air-Sea Interactions in the Western Pacific Warm Pool during WEPOCS	599
M. Nunez, and K. Michael: Satellite Derivation of Ocean-Atmosphere Heat Fluxes in a Tropical Environment	611

EMPIRICAL STUDIES OF ENSO AND SHORT-TERM CLIMATE VARIABILITY

Klaus M. Weickmann: Convection and Circulation Anomalies over the Oceanic Warm Pool during 1981-1982	623
Claire Perigaud: Instability Waves in the Tropical Pacific Observed with GEOSAT	637
Ryuichi Kawamura: Intraseasonal and Interannual Modes of Atmosphere-Ocean System Over the Tropical Western Pacific	649
David Gutzler, and Tamara M. Wood: Observed Structure of Convective Anomalies	659
Siri Jodha Khalsa: Remote Sensing of Atmospheric Thermodynamics in the Tropics	665
Bingrong Xu: Some Features of the Western Tropical Pacific: Surface Wind Field and its Influence on the Upper Ocean Thermal Structure	677
Bret A. Mullan: Influence of Southern Oscillation on New Zealand Weather	687
Kenneth S. Gage, Ben Basley, Warner Ecklund, D.A. Carter, and John R. McAfee: Wind Profiler Related Research in the Tropical Pacific	699
John Joseph Bates: Signature of a West Wind Convective Event in SSM/I Data	711
David S. Gutzler: Seasonal and Interannual Variability of the Madden-Julian Oscillation	723
Marie-Hélène Radenac: Fine Structure Variability in the Equatorial Western Pacific Ocean	735
George C. Reid, Kenneth S. Gage, and John R. McAfee: The Climatology of the Western Tropical Pacific: Analysis of the Radiosonde Data Base	741

Chung-Hsiung Sui, and Ka-Ming Lau: Multi-Scale Processes in the Equatorial Western Pacific	747
Stephen E. Zebiak: Diagnostic Studies of Pacific Surface Winds	757

MISCELLANEOUS

Rick J. Bailey, Helene E. Phillips, and Gary Meyers: Relevance to TOGA of Systematic XBT Errors	775
Jean Blanchot, Robert Le Borgne, Aubert Le Bouteiller, and Martine Rodier: ENSO Events and Consequences on Nutrient, Planktonic Biomass, and Production in the Western Tropical Pacific Ocean	785
Yves Dandonneau: Abnormal Bloom of Phytoplankton around 10°N in the Western Pacific during the 1982-83 ENSO	791
Cécile Dupouy: Sea Surface Chlorophyll Concentration in the South Western Tropical Pacific, as seen from NIMBUS Coastal Zone Color Scanner from 1979 to 1984 (New Caledonia and Vanuatu)	803
Michael Szabados, and Darren Wright: Field Evaluation of Real-Time XBT Systems	811
Pierre Rual: For a Better XBT Bathy-Message: Onboard Quality Control, plus a New Data Reduction Method	823